AJNR

# Diagnostic Value of Increased Diffusion Weighting of a Steady-state Free Precession Sequence for Differentiating Acute Benign Osteoporotic Fractures from Pathologic Vertebral Compression Fractures

Andrea Baur, Armin Huber, Birgit Ertl-Wagner, Roland Dürr, Stefan Zysk, Susanne Arbogast, Michael Deimling and Maximilian Reiser



*AJNR Am J Neuroradiol* 2001, 22 (2) 366-372
http://www.ajnr.org/content/22/2/366

*AJNR Am J Neuroradiol* 22:366–372, February 2001

# Diagnostic Value of Increased Diffusion Weighting of a Steady-state Free Precession Sequence for Differentiating Acute Benign Osteoporotic Fractures from Pathologic Vertebral Compression Fractures

Andrea Baur, Armin Huber, Birgit Ertl-Wagner, Roland Dürr, Stefan Zysk, Susanne Arbogast, Michael Deimling, and Maximilian Reiser

***BACKGROUND AND PURPOSE:*** **Differentiating acute benign from neoplastic vertebral compression fractures can pose a problem in differential diagnosis on routine MR sequences, as signal changes can be quite similar. Our purpose was to assess the value of increasing the diffusion weighting of a diffusion-weighted steady-state free precession (SSFP) sequence for differentiating these two types of vertebral compression fractures.**

***METHODS:*** **Twenty-nine patients with 32 acute vertebral compression fractures caused by osteoporosis (n = 15) or malignancy (n = 17) were examined with a diffusion-weighted SSFP sequence, a T1-weighted spin-echo sequence, and a short-inversion-time inversion recovery sequence. The SSFP sequence was performed with increased diffusion weighting ($\delta$ = 0.6, 3.0, 6.0, and 9.0 ms). The signal intensities of the fractured vertebral bodies were rated on a five-point scale from markedly hypointense to markedly hyperintense relative to normal adjacent vertebral bodies. Quantitative analysis was performed by region-of-interest measurements and by calculating the bone marrow contrast ratio. Statistical analysis was performed with the Mann Whitney *U* test and Student's *t* test.**

***RESULTS:*** **At $\delta$ = 3 ms, the osteoporotic fractures yielded hypointense signal in seven cases, isointense signal in six, and hyperintense signal in two. The fractures showed a progressive signal loss with increased diffusion weighting, so that hypointensity was reached in all but one case. All metastatic fractures had hyperintense signal with $\delta$ = 3 and 6.0 ms. With $\delta$ = 9.0 ms, four fractures became isointense.**

***CONCLUSION:*** **Increasing diffusion weighting can reduce false-positive hyperintense osteoporotic fractures or make hypointensity more obvious in cases of osteoporotic fractures.**

MR diffusion-weighted imaging has became more widely available in recent years. In neuroradiologic settings it is already a well-established method that has proved especially useful in the assessment of acute stroke (1–4). In animal studies, diffusion-weighted imaging has been used to investigate soft-tissue tumors. The method has also been used to differentiate viable from necrotic tumor tissue (5–7). Recently, diffusion-weighted sequences have been proposed as a helpful adjunct in the differentiation of acute benign osteoporotic fractures from pathologic fractures of the spine (8–11). Hypo- or isointense signal intensity in an acute vertebral compression fracture indicates a benign osteoporotic fracture, whereas hyperintensity indicates a metastatic fracture. The purpose of this study was to examine the diagnostic value of increasing the diffusion weighting with the steady-state free precession (SSFP) technique in vertebral compression fractures.

Received November 15, 1999; accepted after revision June 28, 2000.

From the Departments of Diagnostic Radiology (A.B., A.H., B.E-W., M.R.), Orthopaedic Surgery (R.D., S.Z.), and Pathology (S.A.), University of Munich, Germany; and Siemens Medical Systems, Erlangen, Germany (M.D.).

Address reprint requests to Andrea Baur, MD, Department of Diagnostic Radiology, University of Munich, Marchioninistr. 15, 81377 Munich, Germany.



## Methods

We prospectively examined 29 consecutive patients (13 female, 16 male) with 32 vertebral compression fractures. Thirteen patients (mean age, 75 years) had 15 vertebral compression fractures of an acute osteoporotic nature. A fracture was defined as acute when bone marrow edema was apparent on MR examinations. Since traumatic fractures usually do not pose a problem in differential diagnosis, these fracture types were excluded in this study. Confirmation of the diagnosis in

the osteoporotic group was achieved by follow-up MR examinations after more than 3 months in nine patients and by surgical intervention in one case. Surgery was performed in the latter patient because the osteoporotic fracture had led to compression of the spinal canal. In three patients the clinical history ruled out malignancy as the cause of the fracture. All patients had follow-up clinical and radiographic examinations after 1 year.

Sixteen patients (mean age, 62 years) had 17 pathologic vertebral compression fractures. None of these patients had been treated with chemotherapy or radiation therapy. The underlying tumors included breast cancer (n = 4), bronchogenic carcinoma (n = 3), pancreatic carcinoma (n = 1), adenocarcinoma of unknown origin (n = 1), multiple myeloma (n = 1), transitional cell carcinoma (n = 1), renal cell carcinoma (n = 3), prostate cancer (n = 1), and gastric cancer (n = 1). The diagnosis of a pathologic fracture was confirmed by surgery in 11 patients or follow-up MR examinations after 6 months in one patient. In four cases, unequivocal imaging findings in the presence of a primary tumor served as confirmation of the diagnosis. Infiltration of posterior elements plus multifocal metastases in the other vertebrae were rated as unequivocal imaging findings of malignancy. These patients were treated with radiation therapy after MR imaging.

MR imaging was performed using a spinal array surface coil on a 1.5-T MR system. Sagittal T1-weighted spin-echo (SE) images (450/15 or 614/12 [TR/TE]) and short-inversion-time inversion recovery (STIR) images (3600/60, TI = 150 ms) with a 4-mm slice thickness were acquired in all patients (matrix, 256 or 242 × 512; field of view [FOV], 250 × 500 mm). The diffusion-weighted SSFP sequence was performed with the following parameters: TR = 25, matrix = 230 × 256, FOV = 230 mm. The slice position with the most pronounced signal increase on the STIR images was chosen for the diffusion-weighted SSFP sequence. The diffusion weighting was increased from a diffusion pulse length of $\delta = 0.6$ ms (10 acquisitions, 58 seconds) to 3.0 ms (20 acquisitions, 1.56 minutes), 6.0 ms (30 acquisitions, 2.53 minutes), and 9.0 ms (40 acquisitions, 3.51 minutes). The diffusion gradient strength was 23 mT/m. The diffusion gradient of this sequence was applied in the read-out direction (head-feet). In two volunteers and two patients (not included) the diffusion gradient was also applied in phase and slice directions. No anisotropy could be found. It was therefore determined that one direction of the diffusion gradient was adequate for this study.

Owing to the contribution of stimulated- and higher-order echo coherences to the SE, the resulting diffusion weighting is strong even with short diffusion sensitizing gradient pulses. With low flip angles, the diffusion weighting can be increased, because the signal persists longer and experiences more diffusion gradients. The signal generation of the diffusion-weighted SSFP signal is strongly dependent on tissue parameters, such as the T1 and T2 relaxation times and the sequence parameters. Therefore, in principle, each voxel of the image has a different b value. Thus, no global b value can be given and no apparent diffusion coefficient (ADC) maps can be calculated without knowledge of the accurate relaxation maps and flip angle distribution across the slice (12). This is quite different from conventional diffusion-weighted imaging with a Stejskal-Tanner gradient scheme. In this scheme, the b value is well defined by the sequence parameters alone, such as the diffusion gradient strength $G_D$, its length, d, and the diffusion time, D. With the help of the echo-damping factor exp (−bD), an ADC value can be easily calculated from a factorized diffusion-weighted signal.

Two radiologists evaluated the SSFP sequence qualitatively. Image review was performed with respect to the appearance of bone marrow alterations, at first independently and then in a consensual review. On the SSFP images, the signal intensity in the fractured vertebral body was classified as slightly hyper- or hypointense, markedly hyper- or hypointense, or isointense relative to adjacent normal bone marrow. Statistical evaluation of the qualitative analysis between the two groups of fractures was performed with the Mann-Whitney *U* test. Quantitative evaluation was accomplished by region-of-interest (ROI) measurements. The ROIs were placed in the fractured vertebral body, in the adjacent normal vertebral body, and in the background noise. Bone marrow contrast was determined as follows: [SI (abnormal marrow) − SI (normal marrow)]/SI (normal marrow). Statistical analysis was performed by using Student's *t* test. A *P* value less than .01 was considered to indicate a statistically significant difference.

## Results

Vertebral fractures were found from the fifth thoracic to the fifth lumbar vertebral bodies in the osteoporotic group and from the sixth cervical to the fourth lumbar vertebral bodies in the tumor group. In the cases in which follow-up MR examinations were used to confirm the diagnosis of benign fractures, bone marrow edema disappeared completely or was reduced in extension on T1-weighted and STIR images. In the cases of benign vertebral fractures in which the patient's history in combination with follow-up physical examination served as confirmation of the diagnosis, the patients had complete relief of back pain after 1 year. Radiographic examinations in these patients showed an unaltered shape and structure of the vertebral body or signs of healing of the fracture with sclerosis.

The signal intensities of the fractured osteoporotic vertebral bodies on the SSFP sequence ($\delta =$ 3 ms) were hypointense in seven cases, isointense in six cases, and hyperintense in two cases. The six isointense benign fractures and one of the two false-positive hyperintense fractures became hypointense with increased diffusion pulse lengths of 6.0 and 9.0 ms. One osteoporotic fracture remained isointense even at $\delta = 6.0$ and 9.0 ms. At $\delta = 9.0$ ms, the image quality in one patient was rated as nondiagnostic. In the tumor group, the fractured vertebral bodies were hyperintense in all cases with $\delta = 3$ ms. With an increased diffusion pulse length of 6.0 ms, some signal loss could be observed, but all the fractures remained hyperintense. With a diffusion pulse length of 9.0 ms, 11 fractures remained hyperintense and four fractures became isointense. The images in two patients were rated as nondiagnostic at $\delta = 9.0$ ms, and in one patient at $\delta = 6.0$ ms. In general, as known from diffusion-weighted imaging of other areas, the overall signal in the image was reduced with increased diffusion weighting. The signal intensities of the qualitative evaluation of the SSFP sequence with increasing diffusion strength are summarized in the Table. These results were significantly different between the two groups ($P < .001$).

In osteoporotic fractures, the whole vertebral body was iso- or hypointense on SSFP images. A small line or triangle of hyperintensity was seen in two cases. This was located parallel to the fractured endplate and reflected disk tissue that was punched into the vertebral body. In tumorous fractures, the

**Qualitative evaluation of signal intensities of fractured vertebral bodies for osteoporotic and tumorous fractures with increasing δ relative to normal surrounding bone marrow**

| | Signal Intensity | | | | | | | |
|---|---|---|---|---|---|---|---|---|
| | δ = 0.6 ms | | δ = 3.0 ms | | δ = 6.0 ms | | δ = 9.0 ms | |
| Osteoporosis group (n = 15) | ↑↑ | n = 2 | ↑↑ | n = 1 | ↑↑ | n = 0 | ↑↑ | n = 0 |
| | ↑ | n = 2 | ↑ | n = 1 | ↑ | n = 0 | ↑ | n = 0 |
| | ⇔ | n = 9 | ⇔ | n = 6 | ⇔ | n = 1 | ⇔ | n = 1 |
| | ↓ | n = 2 | ↓ | n = 7 | ↓ | n = 9 | ↓ | n = 2 |
| | ↓↓ | n = 0 | ↓↓ | n = 0 | ↓↓ | n = 5 | ↓↓ | n = 11* |
| Tumor group (n = 17) | ↑↑ | n = 16 | ↑↑ | n = 16 | ↑↑ | n = 6 | ↑↑ | n = 1 |
| | ↑ | n = 1 | ↑ | n = 1 | ↑ | n = 10 | ↑ | n = 10 |
| | ⇔ | n = 0 | ⇔ | n = 0 | ⇔ | n = 0 | ⇔ | n = 4 |
| | ↓ | n = 0 | ↓ | n = 0 | ↓ | n = 0 | ↓ | n = 0 |
| | ↓↓ | n = 0 | ↓↓ | n = 0 | ↓↓ | n = 0† | ↓↓ | n = 0† |

Note.—↑↑ indicates markedly hyperintense; ↑, hyperintense; ⇔, isointense; ↓, hypointense; ↓↓, markedly hypointense.

*One δ = 9.0-ms sequence resulted in no signal. Pathologic fractures remained hyperintense with increasingly δ, although some signal loss was noted.

†One δ = 6.0-ms sequence and 2 δ = 9.0-ms sequences resulted in no signal. No overlap of signal intensities in the two groups was seen with a δ = 6-ms sequence.

major parts of the vertebral body were hyperintense.

Quantitative evaluation of the bone marrow contrast at $\delta = 0.6$ ms showed positive values for osteoporotic fractures (mean value, 0.07; SD, 0.52) as well as for tumorous fractures (mean value, 2.78; SD, 1.27). At $\delta = 3$ ms, the mean value of the bone marrow contrast was −0.16 (SD, 0.45) for the osteoporosis group and 2.19 (SD, 1.35) for the tumor group. At $\delta = 6.0$ ms, the bone marrow contrast was −0.55 (SD, 0.42) for the osteoporosis group and 1.65 (SD, 1.62) for the tumor group. At $\delta = 9.0$ ms, the mean value of the bone marrow contrast was −0.70 (SD, 0.35) for osteoporotic fractures and 0.98 (SD, 0.90) for tumorous fractures. These results were all significantly different at a $P$ value of $< .001$ (Fig 1).

Histopathologic specimens obtained in the osteoporotic vertebral fractures showed bone marrow edema with osteoporotic cancellous bone and increased bone turnover. The normal architecture of red bone marrow had disappeared. Hematopoietic and fat cells were reduced and some fibrosis was noted. Histopathologic findings in the tumor group showed the marrow space filled in with cancer cells. The normal hematopoietic marrow was replaced. In three cases, reactive dense fibrosis was apparent.

## Discussion

Differentiating acute benign osteoporotic fractures from spontaneous vertebral compression fractures caused by a malignant lesion poses a distinctive diagnostic problem, since both types of fracture exhibit similar signal changes on routine MR images. Recently, diffusion-weighted MR imaging has shown promising results in solving this diagnostic dilemma (8–11). To date, however, this technique, with step-by-step increases in diffusion weighting, has not been performed in vertebral fractures. Our goal in this study was to assess the diagnostic value of increasing diffusion weighting with an SSFP sequence in patients with acute benign osteoporotic fractures and neoplastic vertebral compression fractures.

The diffusion-weighted SSFP sequence showed a high diagnostic accuracy for differentiating acute benign osteoporotic fractures from pathologic fractures. At $\delta = 3$ ms, hypo- or isointense signal was diagnostic for an acute benign fracture, whereas high signal intensity was suggestive of pathologic bone marrow infiltration. The low signal intensity of acute benign vertebral compression fractures on diffusion-weighted images may be due to bone marrow edema, leading to an increase in the mean free path length of water protons and therefore to a signal loss in the fractured areas. The significantly lower bone marrow contrast and the progressive signal loss with increasing diffusion weighting in osteoporotic fractures support this theory (Table). At $\delta = 3$ ms, six osteoporotic fractures showed isointense signal and two osteoporotic fractures showed hyperintense signal on the diffusion-weighted SSFP sequence. Unfortunately, we have no histopathologic correlation for this finding, although a possible explanation is that bone marrow edema can be quite variable and some reactive fibrosis may cause restriction of diffusion, requiring stronger diffusion weighting. This contention is substantiated by the fact that, except in one patient, the fractured areas became hypointense with a higher diffusion weighting at $\delta = 6.0$ and 9.0 ms (Fig 2). At $\delta = 6.0$ ms, there was no overlap in signal intensities between the two types of fracture (Table).

On the diffusion-weighted SSFP sequence, all pathologic vertebral fractures showed high signal intensity relative to normal bone marrow (Fig 3). The high T2 relaxation time of metastases leads to

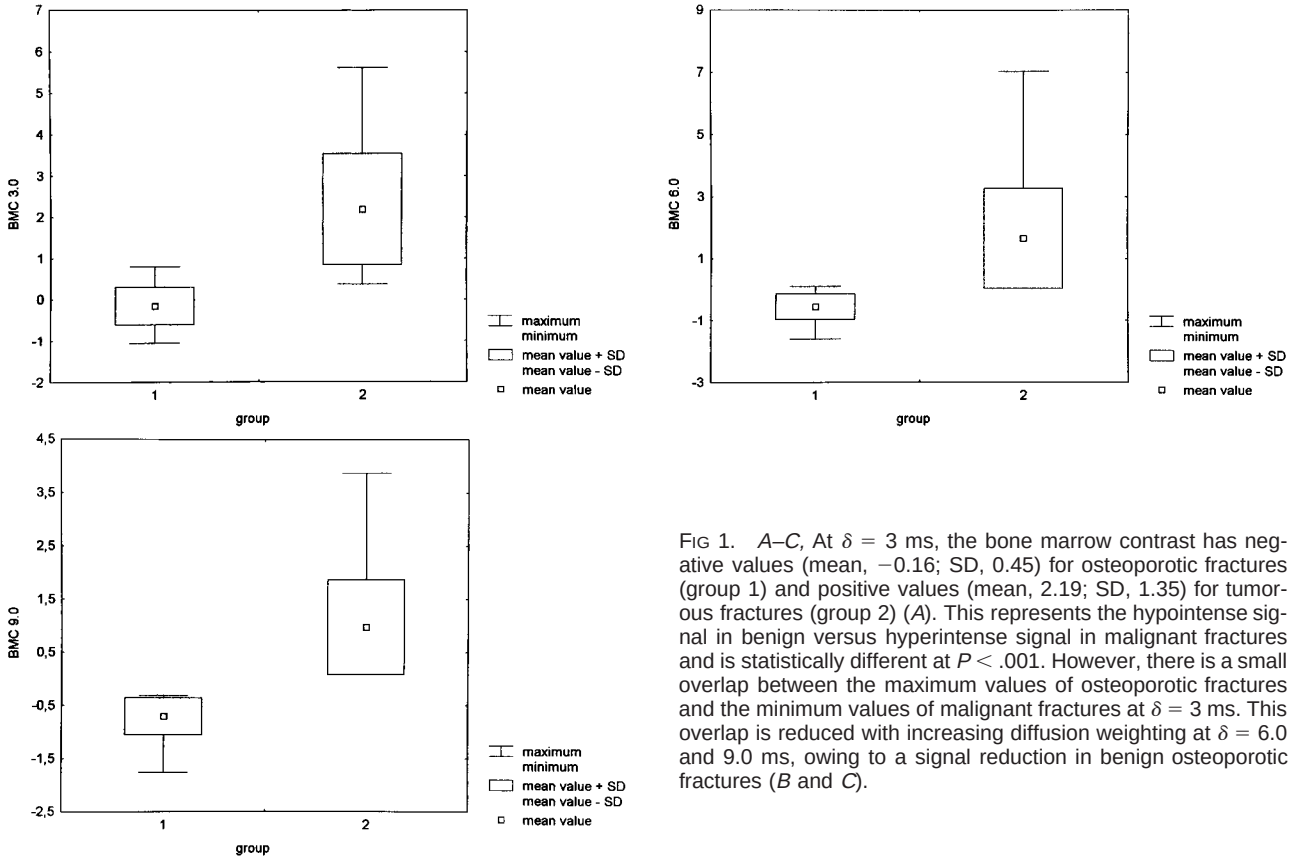


FIG 1. *A–C,* At $\delta = 3$ ms, the bone marrow contrast has negative values (mean, −0.16; SD, 0.45) for osteoporotic fractures (group 1) and positive values (mean, 2.19; SD, 1.35) for tumorous fractures (group 2) (*A*). This represents the hypointense signal in benign versus hyperintense signal in malignant fractures and is statistically different at $P < .001$. However, there is a small overlap between the maximum values of osteoporotic fractures and the minimum values of malignant fractures at $\delta = 3$ ms. This overlap is reduced with increasing diffusion weighting at $\delta = 6.0$ and 9.0 ms, owing to a signal reduction in benign osteoporotic fractures (*B* and *C*).

high signal intensity. Furthermore, as evidenced by the histopathologic specimens, there is a different composition of bone marrow in metastatic fractures, with dense infiltration of malignant cells, which could lead to restricted extracellular diffusion in contrast to bone marrow edema. With increasing diffusion weighting, a signal loss was found in the fractured vertebral bodies; however, these fractures mostly remained hyperintense, even at higher diffusion weighting (Table, Fig 1).

Recently, three studies examining osteoporotic and pathologic vertebral fractures have been reported (9–11). In general, similar results were found. Matoba et al (9), in a study of 12 metastatic and 10 osteoporotic fractures, reported hyperintensity in 10 and isointensity in two of the 12 pathologic vertebral compression fractures and hypo- or isointensity in all 10 of the osteoporotic fractures. The authors also used an SSFP sequence; however, without knowing the precise technique used or the inclusion criteria for the patients, we cannot attempt to explain the discrepancy of the isointensity found in the two pathologic fractures. It is not clearly stated whether the patients had been treated previously. In our experience, pathologic fractures can become hypointense on an SSFP sequence after radiation therapy. This effect might be related to the T2 value of necrotic cancer cells, to the increased signal-to-noise ratio in the adjacent normal vertebral bodies, which have an increased fat content after radiation, or to a different diffusion capacity in necrotic cells as compared with viable tumor tissue. The latter phenomenon has been found in subcutaneously implanted tumors in rats and mice (5–7). Spüntrup et al (10) used a navigated SE and a stimulated echo diffusion-weighted sequence to differentiate benign edema from malignant bone marrow infiltration on a 1.5-T scanner and found that the bone marrow edema caused by osteoporotic or traumatic fractures showed a substantial signal loss on diffusion-weighted images. However, only a minor signal loss was observed for metastatic involvement. Nakagawa et al (11) studied 119 vertebral compression fractures of benign and malignant origin with a diffusion-weighted single-shot echo-planar sequence and found that 92% of the osteoporotic fractures were hypo- or isointense and 95% of the malignant fractures were hyperintense. Four pathologic fractures were not hyperintense because of previous (effective) treatment with chemotherapy.

The principle of diffusion weighting for the differentiation of benign bone marrow edema from malignant infiltration appears to be reproducible with diverse diffusion-weighted MR techniques. The advantages and disadvantages of different diffusion-weighted techniques, SE, SSFP, and echo-planar imaging need to be correlated more directly in further studies. Navigated sequences are more time-consuming, and motion artifacts can influence

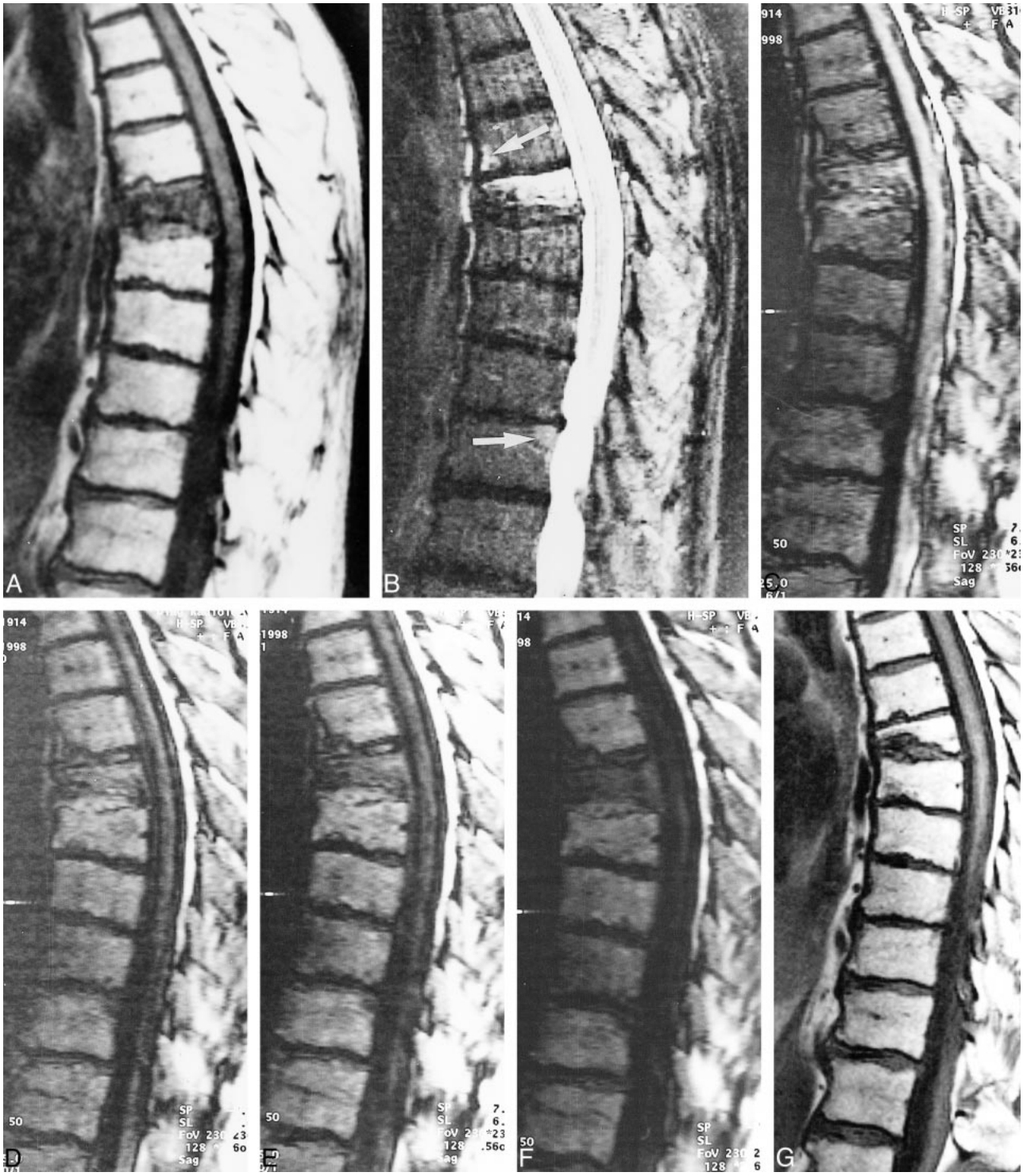


FIG 2. *A,* T1-weighted SE image (450/12) in an 84-year-old man with a compression fracture of the seventh thoracic vertebral body. The fracture occurred in the absence of trauma.

*B,* Complete replacement of the bone marrow space. STIR image (3600/60, TI = 150) shows hyperintensity in the fractured vertebral body. Note also the focal hyperintensities in the sixth thoracic vertebra (*top arrow*) anteriorly and in the 11th thoracic vertebra posteriorly and adjacent to the endplate (*bottom arrow*).

*C,* SSFP sequence with very low diffusion weighting ($\delta$ = 0.6 ms) shows hyperintense signal in the fractured vertebral body.

*D–F,* Increased diffusion weighting with the SSFP sequence (*D* = 3 ms, *E* = 6.0 ms, *F* = 9.0 ms) shows substantial signal loss in the fractured vertebral body. The fractured vertebral body is isointense at $\delta$ = 3 ms and markedly hypointense at $\delta$ = 6.0 and 9.0 ms. The diagnostic value of increased diffusion weighting is the signal loss in benign bone marrow edema. Note that the focal areas of hyperintensity on the STIR images are also hypointense on the SSFP sequence, indicating benign edema.

*G,* Follow-up MR study 8 months later shows healing of the fracture with restitution of fat cells.

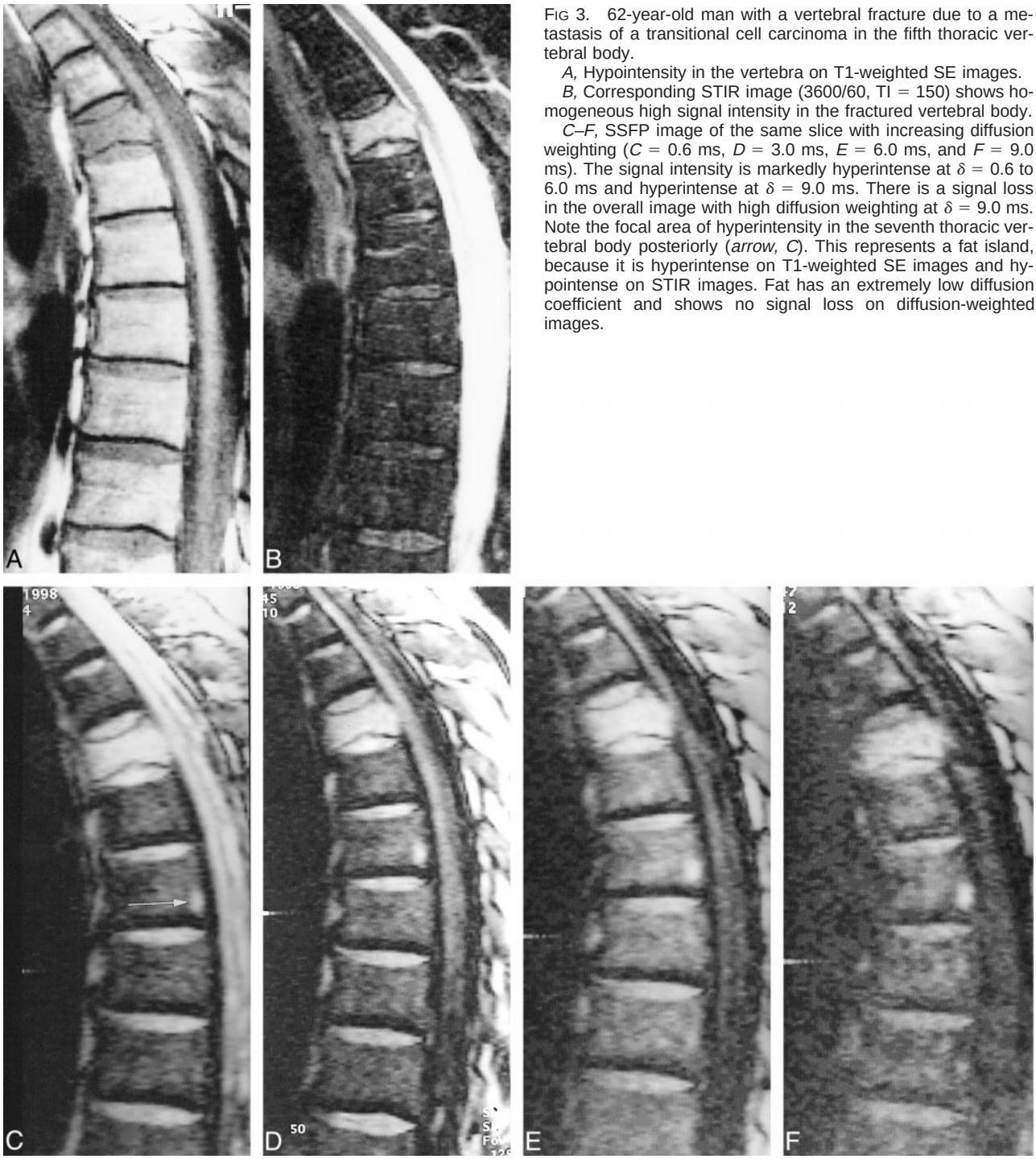


FIG 3. 62-year-old man with a vertebral fracture due to a metastasis of a transitional cell carcinoma in the fifth thoracic vertebral body.

*A,* Hypointensity in the vertebra on T1-weighted SE images.

*B,* Corresponding STIR image (3600/60, TI = 150) shows homogeneous high signal intensity in the fractured vertebral body.

*C–F,* SSFP image of the same slice with increasing diffusion weighting (*C* = 0.6 ms, *D* = 3.0 ms, *E* = 6.0 ms, and *F* = 9.0 ms). The signal intensity is markedly hyperintense at $\delta = 0.6$ to 6.0 ms and hyperintense at $\delta = 9.0$ ms. There is a signal loss in the overall image with high diffusion weighting at $\delta = 9.0$ ms. Note the focal area of hyperintensity in the seventh thoracic vertebral body posteriorly (*arrow, C*). This represents a fat island, because it is hyperintense on T1-weighted SE images and hypointense on STIR images. Fat has an extremely low diffusion coefficient and shows no signal loss on diffusion-weighted images.

image quality, especially in patients with pain (10). On the other hand, signal generation is simpler in SE diffusion weighting, allowing for reliable quantitation of the signal, in contrast to the complicated signal generation of SSFP signals (12–14).

## Conclusion

If the findings on routine T1-weighted SE and STIR images are not completely conclusive for a diagnosis of acute benign or pathologic vertebral compression fracture, then diffusion-weighted imaging of the spine is indicated. At $\delta = 3$ ms, iso- or hypointense signal in the fractured area is indicative of a benign fracture, whereas hyperintense signal indicates a pathologic fracture. If the bone marrow contrast is hyper- or isointense at $\delta = 3$ ms, higher diffusion weighting should be performed with $\delta = 6.0$ ms. At this weighting, an osteoporotic fracture will become hypointense whereas a pathologic fracture will remain hyperintense. Diffusion weighting at $\delta = 9.0$ ms is not recommended, as

image quality sometimes is not diagnostic, even with a large number of acquisitions.

## References


1. Le Bihan D, Breton E, Lallemand D, Grenier P, Cabanis E, Laval-Jeantet M. **MR imaging of intravoxel incoherent motions: application to diffusion and perfusion in neurologic disorders.** *Radiology* 1986;161:401–407
2. Mintorovitch J, Moseley ME, Chileuitt L, Shimizu H, Cohen P, Weinstein PR. **Comparison of diffusion and T2-weighted MRI for the early detection of cerebral ischemia and reperfusion in rats.** *Magn Reson Med* 1991;18:39–50
3. Chien D, Kwong KK, Gress DR, Buonanno FS, Buxton RB, Rosen BR. **MR diffusion imaging of cerebral infarction in humans.** *AJNR Am J Neuroradiol* 1992;13:1097–1102
4. Warach S, Gaa J, Siewert B, Wielopolski P, Edelman RR. **Acute human stroke studied by whole brain echo planar diffusion-weighted magnetic resonance imaging.** *Ann Neurol* 1995;37:231–241
5. Lang P, Wendland MF, Saeed M, et al. **Osteogenic sarcoma: noninvasive in vivo assessment of tumor necrosis with diffusion-weighted MR imaging.** *Radiology* 1998;206:227–235
6. Karczmar GS, River JN, Goldman Z, et al. **Magnetic resonance imaging of rodent tumors using radiofrequency gradient echoes.** *Magn Reson Med* 1994;12:881–893
7. Maier CF, Paran Y, Bendel P, Rutt BK, Degani H. **Quantitative diffusion imaging in implanted human breast tumors.** *Magn Reson Med* 1997;37:576–581
8. Baur A, Stäbler A, Brüning R, et al. **Diffusion-weighted MR imaging of bone marrow: differentiation of benign versus pathologic vertebral compression fractures.** *Radiology* 1998;207:349–356
9. Matoba M, Tonami H, Yokota H, Kuginuki Y, Yamamoto. **Role of diffusion-weighted MRI and P31-MRS in differentiating between malignant and benign vertebral compression fractures.** In: *Book of Abstracts: Society of Magnetic Resonance in Medicine.* Sydney, Australia; 1999:1038
10. Spüntrup E, Adam G, Buecker A, Günther RW. **Navigated spin echo and stimulated echo diffusion-weighted imaging of the spine: potential for differentiation of benign and malignant bone marrow edema.** In: *Book of Abstracts: Society of Magnetic Resonance in Medicine.* Sydney, Australia; 1999:561
11. Nakagawa K, Sakuma H, Ichikawa Y, et al. **Vertebral compression fractures: differentiation between benign and malignant lesions with diffusion-weighted single-shot echo planar MR imaging (abstr).** *Eur Radiol* 2000;10(Suppl 1):154
12. Buxton RB. **The diffusion sensitivity of fast steady-state free precession imaging.** *Magn Reson Imaging* 1993;29:235–243
13. Le Bihan D, Turner R, MacFall JR. **Effects of intravoxel incoherent motions (IVIM) in steady state free precession (SSFP) imaging: application to molecular diffusion imaging.** *Magn Reson Med* 1989;10:324–337
14. Merboldt KD, Haenicke W, Gyngell ML, Frahm J, Bruhn H. **Rapid NMR imaging of molecular self-diffusion using a modified CE-fast sequence.** *J Magn Reson* 1989;82:666